todynamic effects on reactions of coordination complexes; mechanisms derived from such a narrow experimental base must be considered in error.

Acknowledgment. The work described herein was supported by the Office of Basic Energy Sciences of the Department of Energy. This is Document No. NDRL-3180 from the Notre Dame Radiation Laboratory. We also thank Dr. J. F. Endicott, Dr. N. Sutin, and Dr. M. Newton for helpful comments on this work.

Appendix

The approach for calculating orbital and spin restrictions is based on the assumption that, in each particular orientation of the two octahedra, each of the allowed crossings, i.e., one preserving the electronic state symmetry, from the initial to the final electronic state makes a unity contribution to the prohibition factor while each of the forbidden crossings (in a zero order) makes a negligible contribution. The factors must, however, be calculated by dividing the number of effective crossings (crossings with unity contributions) by the total number of crossings, i.e. allowed and forbidden crossings. In these regards, each orientation of the octahedra (Figure 4 and Table II) having a C_{4v} point group symmetry can make only $^1/_9$ contribution according to the orbital prohibition and $^1/_5$ contribution according to the spin prohibition. Indeed, for products with electronic states T_{1g} and T_{2g}, respectively, only one path from E·E (Table II) spans A_1 and correlates, therefore, with an A_1 state of the products. If one uses a similar rationale, a configuration with a C_{2v} point group symmetry contributes $^2/_9$ (orbital contribution) and $^2/_5$ (spin contribution) while one with a C_{3v} point group symmetry contributes $^1/_9$ (orbital contribution) and $^1/_5$ (spin contribution). Insofar as the probability of achieving a given configuration is proportional to the multiplicity of the symmetry preserved in the octahedra collision, the transmission coefficient can be expressed

$$f = \frac{\sum_i n_i o_i \sigma_i}{\sum_i n_i} = \sum_i \frac{n_i}{n} o_i \sigma_i$$

where n_i is the number of configurations preserving a given symmetry element identified by the subscript i, o_i and σ_i are the orbital and spin contributions considered above. Substitution of the values in this expression leads to

$$f = \left[\frac{1}{9} \times \frac{1}{5} \times \frac{2}{5}\right]_{C_{4v}} + \left[\frac{2}{9} \times \frac{2}{5} \times \frac{1}{5}\right]_{C_{2v}} + \left[\frac{1}{9} \times \frac{1}{5} \times \frac{2}{5}\right]_{C_{3v}} \sim \frac{1}{25}$$

Spin–orbit coupling can lift some spin restrictions, and this number must be considered, therefore, a lower limit. Moreover, it is possible to assume that $Co(NH_3)_6^{2+}$ can be generated in its ^2E_g excited state while $Ru(NH_3)_6^{3+}$ is in its ground state.[54] One can calculate $f = ^1/_6$ for such a reaction path with the same rationale discussed above.

Registry No. $Ru(NH_3)_6^{2+}$, 19052-44-9; $Co(NH_3)_6^{3+}$, 14695-95-5; $Co(NH_3)_5Cl^{2+}$, 14970-14-0; $Co(en)_3^{3+}$, 14878-41-2; $Co(sep)^{2+}$, 63218-22-4.

Contribution from the Department de Quimica Inorgànica, Universitat de València, 46100-Burjassot (València), Spain, and Laboratoire de Chimie Inorganique, Unité de Recherche Associée au CNRS No. 420, Université de Paris-Sud, 91405 Orsay, France

Molecular Topology and Exchange Interaction: Synthesis and Magnetic Properties of $[Cu^{II}_3M^{II}]$ (M = Cd, Ni, Mn) Tetranuclear Species

Francesc Lloret,*[1a] Yves Journaux,*[1b] and Miguel Julve[1a]

Received September 9, 1989

Three tetranuclear complexes of formulas $[\{Cu(oxpn)\}_3Cd](NO_3)_2\cdot 2H_2O$, $[Cu_3Cd]$, $[\{Cu(oxpn)\}_3Ni](ClO_4)_2\cdot 2H_2O$, $[Cu_3Ni]$, and $[\{Cu(oxpn)\}_3Mn](ClO_4)_2\cdot 2H_2O$, $[Cu_3Mn]$, where $oxpn^{2-}$ is *N,N'*-bis(3-aminopropyl)oxamidato have been synthesized. Magnetic susceptibility and EPR measurements in the 4.2–3.00 K temperature range have been carried out for this series of complexes. The magnetic data have been interpreted by using the Heisenberg Hamiltonian and lead to J values equal to −1.45, −101.0, and −26.6 cm^{-1} for $[Cu_3Cd]$, $[Cu_3Ni]$, and $[Cu_3Mn]$. The relation between the local **g** tensor and the observed average g values is analyzed. A discussion about the relative interaction intensity in such a series of complexes is presented. Finally, the nature of the ground state is discussed in relation to the topology and the spin values of the metal ions.

Introduction

A lot of work has been devoted to the study of the exchange interaction in polymetallic systems. One of the challenges of this field is the design of complexes with predicted magnetic properties.[2] To achieve this goal, the influence of parameters such as the symmetry of magnetic orbitals,[3,4] the nature of the bridging or terminal ligands,[2,5-6] and small geometrical changes[8,9] has been studied. Surprisingly, no study of the influence of the molecular topology on the magnetic properties of inorganic complexes has been done. On the other hand, organic chemists attempting to synthesize high-spin molecules have been extremely interested in this subject.[10,11] For instance, it is well-known that the trimethylenemethane biradical has a triplet ground state due to its topology.[10,12] A similar topology for inorganic complexes is scarce although the diamagnetic Werner brown salt $[Co\{(OH)_2Co(en)_2\}_3]^{6+}$[13] where en is 1,2-diaminoethane has been known since 1907. The synthesis of the chromium analogue of Werner's complex by Andersen and Berg a few years ago[14a,b] provided

(1) (a) Universitat de València. (b) Université de Paris-Sud.
(2) (a) *Magneto-Structural Correlations in Exchange Coupled Systems*; Willett, R. D., Gatteschi, D., Kahn, O., Eds.; NATO ASI Series; D. Reidel Publishing Co.: Dordrecht/Boston/Lancaster, 1985. (b) Kahn, O. *Angew. Chem., Int. Ed. Engl.* **1985**, *24*, 834 and references therein.
(3) (a) Journaux, Y.; Kahn, O.; Zarembowitch, J.; Galy, J.; Jaud, J. *J. Am. Chem. Soc.* **1983**, *105*, 7585. (b) Kahn, O.; Galy, J.; Journaux, Y.; Jaud, J.; Morgenstern Badarau, I. *J. Am. Chem. Soc.* **1982**, *104*, 2165.
(4) Yu, P.; Journaux, Y.; Kahn, O. *Inorg. Chem.* **1989**, *28*, 100.
(5) See: Hendrickson, D. N. In ref 2a, p 523 ff.
(6) Verdaguer, M.; Kahn, O.; Julve, M.; Gleizes, A. *Nouv. J. Chem.* **1985**, *9*, 325.
(7) (a) Journaux, Y.; Sletten, J.; Kahn, O. *Inorg. Chem.* **1985**, *24*, 4063. (b) Julve, M.; Verdaguer, M.; Kahn, O.; Gleizes, A.; Philoche-Levisalles, M. *Inorg. Chem.* **1984**, *23*, 3808. (c) Lloret, F.; Julve, M.; Faus, J.; Journaux, J.; Philoche-Levisalles, M.; Jeannin, Y. *Inorg. Chem.* **1989**, *28*, 3702.
(8) (a) Crawford, W. H.; Richardson, H. W.; Wasson, J. R.; Hodgson, D. J.; Hattfield, W. E. *Inorg. Chem.* **1976**, *15*, 2107. (b) See: Hodgson, D. J. In ref 2, p 497 ff. (c) Livermore, J. C.; Willett, R. D.; Gaura, R. M.; Landee, C. P. *Inorg. Chem.* **1982**, *21*, 1403.
(9) (a) Hay, P. J.; Thibeault, J. C.; Hoffmann, R. *J. Am. Chem. Soc.* **1975**, *97*, 4884. (b) Charlot, M. F.; Jeannin, S.; Jeannin, Y.; Kahn, O.; Lucrece Abaul, J.; Martin Frere, J. *Inorg. Chem.* **1979**, *18*, 1675.
(10) Ovchinnikov, A. *Theor. Chim. Acta* **1978**, *47*, 297.
(11) Mataga, N. *Theor. Chim. Acta* **1968**, *10*, 372.
(12) Dowd, P. *Acc. Chem. Res.* **1972**, *5*, 242.
(13) (a) Werner, A. *Ber. Dtsch. Chem. Ges.* **1907**, *40*, 2103. (b) Thewalt, U. *Chem. Ber.* **1971**, *104*, 2657.

0020-1669/90/1329-3967$02.50/0

magnetochemists with a more exciting complex. This compound exhibits a high-spin $S = 3$ ground state owing to its topology.[14c] In the framework of the Ising model, the biradical and the chromium complex have the same ground-state spin structure:

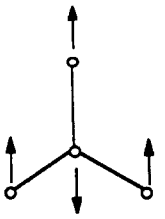

Nevertheless, they exhibit a different ground-state spin multiplicity due to their different local spin values ($^1/_2$ for the biradical and $^3/_2$ for the chromium complex).

This article is devoted to another example of complexes exhibiting the same topology. We report on the synthesis and magnetic properties of three tetranuclear complexes of formulas $[\{Cu(oxpn)\}_3Cd](NO_3)_2 \cdot 2H_2O$, $[Cu_3Cd]$, $[\{Cu(oxpn)\}_3Ni](ClO_4)_2 \cdot 2H_2O$, $[Cu_3Ni]$, and $[\{Cu(oxpn)\}_3Mn](ClO_4)_2 \cdot 2H_2O$, $[Cu_3Mn]$, where $oxpn^{2-} = N,N'$-bis(3-aminopropyl)oxamidato. The $[Cu_3Ni]$ complex has been studied already by Okawa et al.[15]

Experimental Section

Materials. Cadmium(II) nitrate tetrahydrate, nickel(II) perchlorate hexahydrate, and manganese(II) perchlorate hexahydrate were purchased from Aldrich and used as received. Cu(oxpn) and H_2oxpn were synthesized according to previously reported procedures.[7a,16] The syntheses of the tetranuclear complexes were carried out under an argon atmosphere in order to avoid both CO_2 uptake by the solutions and Mn(II) oxidation. All our attempts to obtain single crystals were unsuccessful.

$[\{Cu(oxpn)\}_3Cd](NO_3)_2 \cdot 2H_2O$, $[Cu_3Cd]$. A 0.5-mmol amount of cadmium(II) nitrate dissolved in 10 mL of methanol was added to a methanolic suspension (20 mL) of 1.5 mmol of Cu(oxpn). The resulting violet solution was filtered, and the filtrate was allowed to stand until violet crystals of $[Cu_3Cd]$ separated out. Its perchlorate salt as a dihydrate was synthesized by following a similar procedure but in aqueous solution. It was obtained as a violet polycrystalline powder by slow evaporation after adding sodium perchlorate in excess. Anal. Calcd for $C_{24}H_{52}N_{14}O_{14}Cu_3Cd$, $[Cu_3Cd]$: C, 27.11; H, 4.89; N, 18.44. Found: C, 27.30; H, 4.86; N, 18.45.

$[\{Cu(oxpn)\}_3Ni](ClO_4)_2 \cdot 2H_2O$, $[Cu_3Ni]$. A 0.5-mmol amount of nickel(II) perchlorate dissolved in 10 mL of acetonitrile was added to a suspension of 1.5 mmol of Cu(oxpn) in 20 mL of acetonitrile. The purple solution thus obtained was filtered, and violet crystals of $[Cu_3Ni]$ were obtained by slow evaporation. Anal. Calcd for $C_{24}H_{52}N_{12}O_{16}Cl_2Cu_3Ni$, $[Cu_3Ni]$: C, 26.56; H, 4.84; N, 15.49; Cl, 6.53; Cu, 17.57; Ni, 5.41. Found: C, 26.65; H, 4.75; N, 15.54; Cl, 6.71; Cu, 17.50; Ni, 5.45.

$[\{Cu(oxpn)\}_3Mn](ClO_4)_2 \cdot 2H_2O$, $[Cu_3Mn]$. This compound was obtained as described above for $[Cu_3Ni]$ by substituting Mn(II) perchlorate for Ni(II) perchlorate. Anal. Calcd for $C_{24}H_{52}N_{12}O_{16}Cl_2Cu_3Mn$, $[Cu_3Mn]$: C, 26.66; H, 4.85; N, 15.55; Cl, 6.56; Cu, 17.63; Mn, 5.08. Found: C, 26.75; H, 4.72; N, 15.56; Cl, 6.82; Cu, 17.50; Mn, 5.20.

Physical Measurements. Infrared spectra of KBr pellets were taken on a Perkin-Elmer 1750 FTIR spectrophotometer. Diffuse-reflectance spectra of Nujol mulls on filter paper were recorded with a Perkin-Elmer Lambda 9 spectrophotometer.

Magnetic measurements were carried out on polycrystalline samples with a Faraday-type magnetometer equipped with a helium continuous-flow cryostat working in the 4.2–300 K temperature range. The susceptibility independence of the applied field was checked at room temperature for all compounds. Mercury tetrakis(thiocyanato)cobaltate(II) was used as a susceptibility standard. Diamagnetic corrections were estimated as -471×10^{-6}, -488×10^{-6}, and -490×10^{-6} cm^3 mol^{-1} for $[Cu_3Cd]$, $[Cu_3Ni]$, and $[Cu_3Mn]$.

EPR spectra were recorded on powder samples at X-band frequency with a Bruker ER200D spectrometer equipped with an Oxford Instruments continuous-flow cryostat working in the 4.2–300 K temperature range. The magnetic field and the klystron frequency were determined with a Hall probe and a Hewlett Packard frequency meter.

Table I. Absorption Maxima and Magnetic Data for Complexes $[Cu_3M]$

M	$10^{-3}\nu_{max}$, cm^{-1}	J, cm^{-1}	g_{Cu}	g_M	10^5R^a
Cd	28.6, 18.9	−1.45	2.04		33.0
Ni	27.0, 18.9, 13.3 sh, 8.6	−101.0	2.16	2.19	0.68
Mn	26.7, 24.4, 18.9	−26.6	1.99	1.98	3.1

$^a R = \sum[(\chi_M T)^{obs} - (\chi_M T)^{calc}]^2 / \sum[(\chi_M T)^{obs}]^2$.

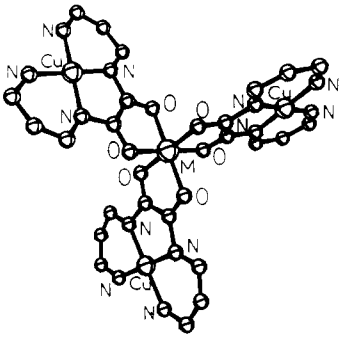

Figure 1. Proposed molecular structure of the $[Cu_3M]$ tetranuclear species.

Results

IR and Electronic Spectra. The three tetranuclear complexes (perchlorate series) display identical IR spectra. The most relevant feature is the presence of the ν(N–C–O) stretching bands around 1600 and 1450 cm^{-1}, which are characteristic of the bridging oxamido group.[17] On the other hand the δ(CO) deformation peak, which is centered at 710 cm^{-1} for the complex Cu(oxpn), is not observed in the spectra of the tetranuclear complexes. This fact has been attributed to the coordination of the carbonyl oxygen atoms to metal ions.[15]

The band maxima of the reflectance spectra of $[Cu_3Cd]$, $[Cu_3Ni]$, and $[Cu_3Mn]$ are listed in Table I together with the magnetic results. All the spectra show a band centered at 18 900 cm^{-1}, which is tentatively assigned to the d–d transition in coordinated Cu(oxpn). This band is shifted to 20 400 cm^{-1} in free Cu(oxpn), which is consistent with the expected decrease of the ligand field for coordinated Cu(oxpn) when compared with free Cu(oxpn). Such d–d transitions at fairly high energies, 18 900 and 20 400 cm^{-1} for $[Cu_3Cd]$, $[Cu_3Ni]$, $[Cu_3Mn]$, and noncoordinated Cu(oxpn), suggest nearly square-planar coordination[18] in each case. The high-energy absorptions at 28 600, 27 000, and 26 700 cm^{-1} for $[Cu_3Cd]$, $[Cu_3Ni]$, and $[Cu_3Mn]$, respectively, are due to metal–ligand charge-transfer bands. The corresponding absorption for noncoordinated Cu(oxpn) appears at 28 200 cm^{-1}, a value which is very close to the one observed for $[Cu_3Cd]$. The broad absorption at 8600 cm^{-1} and the shoulder at 13 300 cm^{-1} in $[Cu_3Ni]$ spectra are attributed to the $^3A_{2g} \rightarrow {}^3T_{2g}$ and $^3A_{2g} \rightarrow {}^3T_{1g}(F)$ transitions of octahedral nickel(II). The third transition, $^3A_{2g} \rightarrow {}^3T_{1g}(P)$, is obscured by charge-transfer bands. The resulting $10Dq$ value for this complex ($10Dq = 8600$ cm^{-1}) is very close to the reported value for $[Ni(H_2O)_6]^{2+}$ ($10Dq = 8500$ cm^{-1}).[19] The sharp band centered at 24 400 cm^{-1} in the spectra of $[Cu_3Mn]$ is attributable to the $^6A_{1g} \rightarrow {}^4E_g$ spin-forbidden transition of manganese(II).[20] Spectroscopic results together with analytical data and magnetic and EPR studies (vide infra) strongly support the proposed structure of the tetranuclear species schematized in Figure 1.

Magnetic Properties. $[Cu_3Cd]$. The $\chi_M T$ versus T plot $[Cu_3Cd]$ is shown in Figure 2. Down to 150 K, the $\chi_M T$ product is constant

(14) (a) Andersen, P.; Berg, T. *J. Chem. Soc., Chem. Commun.* **1974**, 601. (b) Andersen, P.; Berg, T. *Acta Chem. Scand., Ser. A* **1978**, *32*, 989. (c) Gudel, H.; Hauser, U. *Inorg. Chem.* **1980**, *19*, 1325.
(15) Okawa, H.; Kawahara, Y.; Mykuriya, M.; Kida, S. *Bull. Chem. Soc. Jpn.* **1980**, *53*, 549.
(16) Chang, H. J.; Volg, A. *J. Polym. Sci., Polym. Chem. Ed.* **1977**, *15*, 311.
(17) Ojima, H.; Nonoyama, K. *Z. Anorg. Allg. Chem.* **1972**, *389*, 75.
(18) Hataway, B. J. *J. Chem. Soc., Dalton Trans.* **1972**, 1196.
(19) Drago, R. S. *Physical Methods in Chemistry*; Saunders Co.: Philadelphia, PA, 1977; p 382.
(20) Lever, A. B. P. *Inorganic Electronic Spectroscopy*, 2nd ed.; Elsevier: Amsterdam, 1986; p 448.

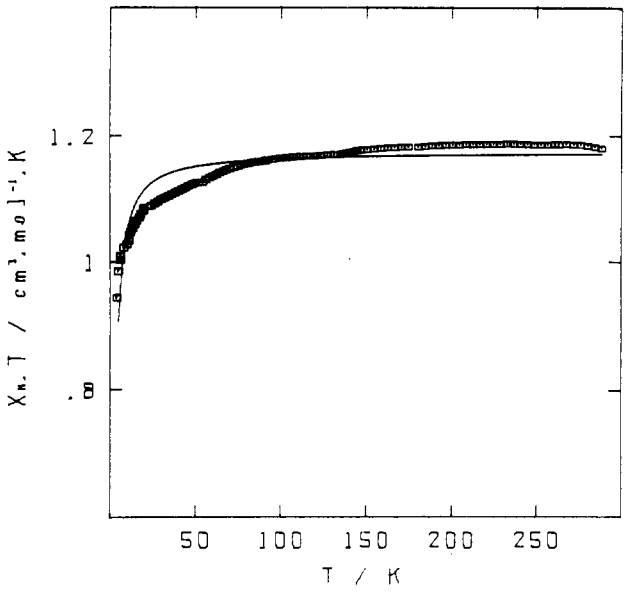

Figure 2. Experimental (□) and calculated (—) temperature dependences of $\chi_M T$ for [Cu_3Cd].

and equal to 1.19 $cm^3\ mol^{-1}\ K$. Below 150 K, $\chi_M T$ decreases slightly and reaches 0.94 $cm^3\ mol^{-1}\ K$ at 4.2 K. Such a decrease can be due to either intra- or intermolecular interactions. An upper limit of the doublet–quartet gap arising from the intramolecular interaction between the three Cu(II) ions is obtained by fitting the magnetic data with the theoretical law for an equilateral triangular arrangement derived from the Hamiltonian

$$\hat{H} = -J(\hat{S}_{A1}\hat{S}_{A2} + \hat{S}_{A2}\hat{S}_{A3} + \hat{S}_{A3}\hat{S}_{A1}) + \beta\vec{H}(g_{A1}\hat{S}_{A1} + g_{A2}\hat{S}_{A2} + g_{A3}\hat{S}_{A3}) \quad (1)$$

with $g_{A1} = g_{A2} = g_{A3} = g$, which leads to

$$\chi_M T = \frac{N\beta^2 g^2}{k}\,\frac{1 + 5e^{3J/2kT}}{4 + 4e^{3J/2kT}} \quad (2)$$

The minimization of $R = \sum[(\chi_M T)^{obs} - (\chi_M T)^{calc}]^2/\sum[(\chi_M T)^{obs}]^2$ by a Simplex method leads to $J = -1.45\ cm^{-1}$ and $g = 2.04$ with $R = 3.3 \times 10^{-4}$.

[Cu_3Ni]. The $\chi_M T$ versus T plot of [Cu_3Ni] is shown in Figure 3. At room temperature the $\chi_M T$ value is 1.68 $cm^3\ mol^{-1}\ K$, and it decreases upon cooling. These features are indicative of an antiferromagnetic interaction between the Cu(II) and Ni(II) ions. The $\chi_M T$ product presents a plateau in the 25–4.2 K temperature range with $\chi_M T = 0.433\ cm^3\ mol^{-1}\ K$, as expected for a spin-doublet state. The experimental data were fitted by using the theoretical expression deduced from the spin Hamiltonian

$$\hat{H} = -J(\hat{S}_{A1}\hat{S}_B + \hat{S}_{A2}\hat{S}_B + \hat{S}_{A3}\hat{S}_B) + \beta\vec{H}[g_A(\hat{S}_{A1} + \hat{S}_{A2} + \hat{S}_{A3}) + g_B\hat{S}_B] \quad (3)$$

with A = Cu, B = Ni, and g_A and g_B being the average values of the local g factors. The other symbols have their usual meaning. Defining $\hat{S}^* = \hat{S}_{A1} + \hat{S}_{A2} + \hat{S}_{A3}$, the previous Hamiltonian can be expressed as $\hat{H} = -J\hat{S}^*\hat{S}_B + \beta\vec{H}(g_A\hat{S}^* + g_B\hat{S}_B)$, which leads, in zero field, to the following energy spectrum:

$$E = -J\frac{S(S+1) - S_B(S_B+1) - S^*(S^*+1)}{2} \quad (4)$$

From this spectrum the susceptibility is deduced as

$$\chi_M T = X/Y \quad (5)$$

where

$$X = \tfrac{1}{2}g_{1/2,3/2}{}^2 + \left(g_{1/2,1/2}{}^2 + 5g_{3/2,3/2}{}^2\right)e^{3J/2kT} + 10g_{3/2,1/2}{}^2e^{3J/kT} + \tfrac{35}{2}g_{5/2,3/2}{}^2e^{4J/kT} \quad (6)$$

and

$$Y = 2 + 8e^{3J/2kT} + 8e^{3J/kT} + 6e^{4J/kT} \quad (7)$$

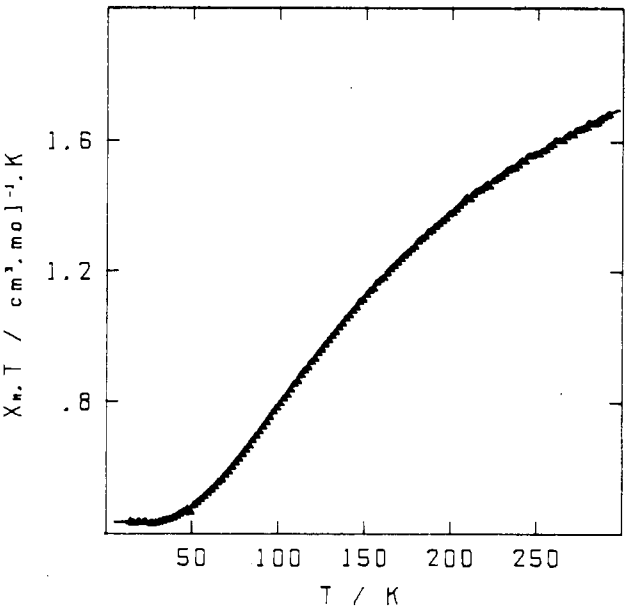

Figure 3. Experimental (△) and calculated (—) temperature dependences of $\chi_M T$ for [Cu_3Ni].

Assuming that the local g factors are isotropic and that $D_{Ni} \ll |J|$, the $g(S,S^*)$ factors are related to g_{Cu} and g_{Ni} by

$$g(S,S^*) = \{g_A[S(S+1) + S^*(S^*+1) - S_B(S_B+1)] + g_B[S(S+1) - S^*(S^*+1) + S_B(S_B+1)]\}/2S(S+1) \quad (8)$$

We have neglected the local anisotropy of the Ni(II) ion as well as the interaction between the Cu(II) ions ($J \approx -1.4\ cm^{-1}$; see [Cu_3Cd] section). Least-squares fitting of the experimental data leads to $J = -101.0\ cm^{-1}$, $g_{Cu} = 2.16$, and $g_{Ni} = 2.19$ with $R = 6.83 \times 10^{-6}$. The observed J value ($-101.0\ cm^{-1}$) for the coupling between the Cu and Ni ions of [Cu_3Ni] is large compared with the zero-field splitting of octahedral Ni(II)($|D| \leq 10\ cm^{-1}$), which anyway has no first-order effect on the ground state. Therefore the initial assumptions of the fit are valid.

[Cu_3Mn]. The $\chi_M T$ versus temperature plot of [Cu_3Mn] is shown in Figure 4. At room temperature its value is 4.63 $cm^3\ mol^{-1}\ K$. Upon cooling, the $\chi_M T$ value steadily decreases to a temperature of 7 K, showing that an antiferromagnetic interaction between the copper and manganese ions is operative. In the 7–4.2 K temperature range the $\chi_M T$ plot exhibits a plateau at 0.981 $cm^3\ mol^{-1}\ K$ corresponding to a triplet state. The experimental data were fitted by using the theoretical expression deduced from the Hamiltonian (3) with A = Cu and B = Mn. This expression is

$$\chi_M T = Z/W \quad (9)$$

with

$$Z = 2g_{1,3/2}{}^2 + 10g_{2,3/2}{}^2e^{2J/kT} + 20g_{2,1/2}{}^2e^{7J/2kT} + 28g_{3,3/2}{}^2e^{5J/kT} + 56g_{3,1/2}{}^2e^{13J/2kT} + 60g_{4,3/2}{}^2e^{9J/kT} \quad (10)$$

and

$$W = 3 + 5e^{2J/2kT} + 10e^{7J/2kT} + 7e^{5J/kT} + 14e^{13J/2kT} + 9e^{9J/kT} \quad (11)$$

The $g(S,S^*)$ values are deduced from eq 8 with A = Cu and B = Mn. We have neglected the influence of the Mn(II) ion local anisotropy as well as the anisotropic exchange in the spin-triplet ground state. This approximation is supported by the fact that there is no evidence in the magnetic data of any deviation from the Curie law at low temperature and by the observation of an EPR spectrum for [Cu_3Mn] (see EPR section). The minimization of R leads to $J = -26.6\ cm^{-1}$, $g_{Cu} = 1.99$, and $g_{Mn} = 1.98$ with $R = 3.13 \times 10^{-5}$.

EPR Spectra. [Cu_3Cd]. The X-band powder spectra of [Cu_3Cd] and Cu(oxpn) at 17 and 4.2 K are represented in Figure 5. The

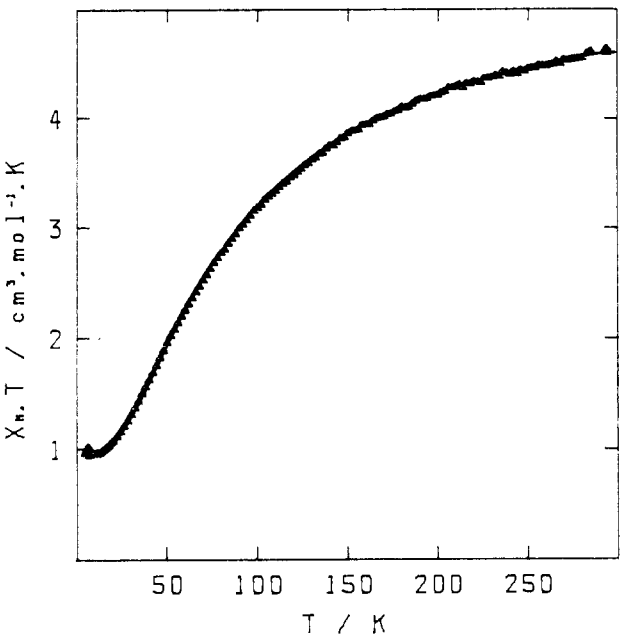

Figure 4. Experimental (△) and calculated (—) temperature dependences of $\chi_M T$ for $[Cu_3Mn]$.

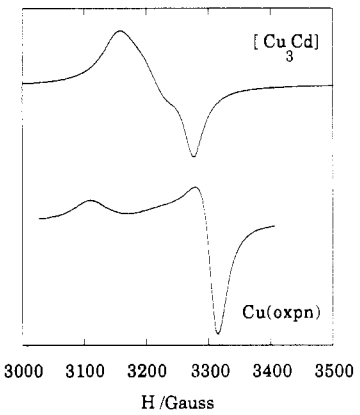

Figure 5. X-Band powder EPR spectra of $[Cu_3Cd]$ (top) and [Cu(oxpn)] (bottom) at 17 and 4.2 K, respectively.

spectrum of $[Cu_3Cd]$ presents rhombic symmetry with g values equal to 2.06, 2.09, and 2.13. There is no evidence of transition ascribable to the excited quartet state. It is obvious from Figure 5 that this spectrum is not the superposition of those of the monomeric fragments (g values equal to 2.05 and 2.17). This indicates that the exchange interaction is operative. The diagonalization of the matrix obtained from the Zeeman Hamiltonian $\hat{H} = \beta\vec{H}(g_{A1}\hat{S}_{A1} + g_{A2}\hat{S}_{A2} + g_{A3}\hat{S}_{A3})$ established on the basis of the ^2E degenerate doublet ground state wave functions leads to the **g** tensors

$$\mathbf{g}_{\pm} = \frac{g_{A1} + g_{A2} + g_{A3}}{3} \pm \frac{2}{3}\sqrt{g_{A1}^2 + g_{A2}^2 + g_{A3}^2 - g_{A1}g_{A2} - g_{A1}g_{A3} - g_{A2}g_{A3}} \quad (12)$$

The EPR spectrum of Cu(oxpn) of Figure 5 indicates that the local $\mathbf{g}_{Cu}$ tensors are axial. Assuming D_3 symmetry for $[Cu_3Cd]$, the local $\mathbf{g}_{Cu}$ tensors are then related by the symmetry axis. From rotation matrices and the transformation formula $g' = RgR^{-1}$, the $\mathbf{g}_{Cu}$ tensors can be expressed on the same basis (principal axis of site A1, for instance) as

$$\mathbf{g}_{A\nu} = \begin{vmatrix} g_i & 0 & 0 \\ 0 & g_j & 0 \\ 0 & 0 & g_k \end{vmatrix} \quad (13)$$

with $\nu = 1$–3 and $i = j = \perp$ and $k = \parallel$ for site A1, $i = k = \perp$ and $j = \parallel$ for site A2, and $j = k = \perp$ and $i = \parallel$ for site A3. From

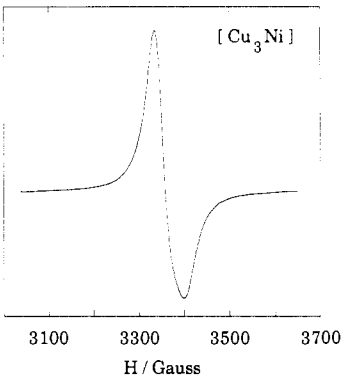

Figure 6. X-Band powder EPR spectrum of $[Cu_3Ni]$ at 18 K.

formula 12 the **g** tensors of the doublet state can be calculated as

$$\mathbf{g}_+ = \begin{vmatrix} g_\parallel & 0 & 0 \\ 0 & g_\parallel & 0 \\ 0 & 0 & g_\parallel \end{vmatrix} \qquad \mathbf{g}_- = \begin{vmatrix} \frac{4g_\perp - g_\parallel}{3} & 0 & 0 \\ 0 & \frac{4g_\perp - g_\parallel}{3} & 0 \\ 0 & 0 & \frac{4g_\perp - g_\parallel}{3} \end{vmatrix} \quad (14)$$

These tensors are isotropic. The apparent rhombicity observed in the experimental spectrum could be due to the superposition of the two close isotropic signals.

Another possible explanation of the rhombicity of the experimental spectrum is the zero-field splitting of the ^2E degenerate doublet state under spin–orbit coupling interaction[21,22] or vibronic interaction.[23] It follows from general theoretical considerations that since there is no representation in the D_3 double group greater than 2-, a 4-fold degeneracy cannot exist. The spin–orbit coupling, which is active on the ^2E ground state, leads to two Kramers doublets, even for undistorted D_3 configuration. The zero-field and Zeeman splittings could take values of the same order of magnitude.[21] The zero-field splitting value is too small to be detected by susceptibility measurement but could lead to the observed experimental spectrum.

$[Cu_3Ni]$. The X-band spectrum of $[Cu_3Ni]$ at 18 K, shown in Figure 6, exhibits an asymmetric line shape that is typical of a slightly anisotropic doublet state with $g_\perp > g_\parallel$. The average g value is 2.019. No new transition is observed upon warming. By the use of vector coupling models[24,25] the $g(S,S^*)$ values can be related to local g factors by

$$g(S,S^*) = \{g_{S^*}[S(S+1) + S^*(S^*+1) - S_B(S_B+1)] + g_B[S(S+1) - S^*(S^*+1) + S_B(S_B+1)]\}/2S(S+1) \quad (15)$$

For the doublet ground state of $[Cu_3Ni]$ this expression leads to

$$g_{1/2,3/2} = \frac{5(g_{Cu1} + g_{Cu2} + g_{Cu3}) - 6g_{Ni}}{9} \quad (16)$$

The average g values for a square-planar Cu(II) and octahedral Ni(II) are approximately $g_{Cu} \approx 2.1$ and $g_{Ni} \approx 2.2$, respectively. Owing to the minus sign in expression 16, one can expect an average g value less than 2.1. The experimental average g value of 2.019 is in good agreement with the predicted one. Since the **g** tensor for Ni(II) is generally isotropic and the tensor g_{Cu1} +

(21) Belinskii, M. I.; Tsukerblat, B. S.; Ablov, A. V. *Mol. Phys.* **1974**, *28*, 283.
(22) (a) Tsukerblat, B. S.; Belinskii, M. I.; Ablov, A. V. *Dokl. Akad. Nauk SSSR* **1971**, *201*, 1410. (b) Tsukerblat, B. S.; Ya Kuyavskaya, B.; Belinskii, M. I.; Ablov, A. V.; Novotortsev, V. M.; Kalinnikov, V. T. *Theor. Chim. Acta* **1975**, *38*, 131.
(23) Jones, D. H.; Sams, J. R.; Thompson, R. C. *J. Chem. Phys.* **1984**, *81*, 440.
(24) (a) Chao, C. C. *J. Magn. Res.* **1973**, *10*, 1. (b) Scaringe, R. P.; Hodgson, D.; Hattfield, W. E. *Mol. Phys.* **1978**, *35*, 701.
(25) See: Gatteschi, D.; Bencini, A. In ref 2a, p 241.

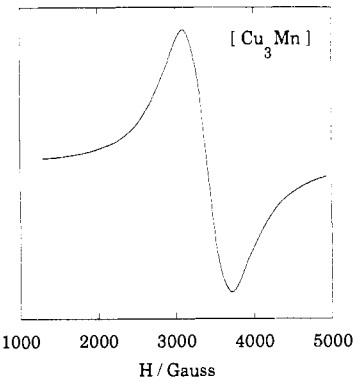

Figure 7. X-Band powder EPR spectrum of [Cu_3Mn] at 6 K.

$g_{Cu2} + g_{Cu3}$ is also isotropic assuming D_3 symmetry, the anisotropy of the experimental spectrum is expected to be very small as observed.

[Cu_3Mn]. The X-band spectrum of [Cu_3Mn] at 6 K is shown in Figure 7. It presents one broad signal centered at $g = 1.987$, indicating that the fine structure of the triplet ground state is less than the incident quantum ($D \ll h\nu$). There is no evidence for any half-field transition, and no new transition is observed upon warming. From eq 15 the triplet ground state g factor is

$$g_{1,3/2} = \frac{7g_{Mn} - (g_{Cu1} + g_{Cu2} + g_{Cu3})}{4} \qquad (17)$$

Taking into account the minus sign in formula 17 and the fact that the g value for a Mn(II) ion is usually close to 2 and that of Cu(II) is approximately 2.1, it is not surprising to find a g factor less than 2 for the triplet ground state.

Discussion

It is now well established that bis-bidentate ligands like

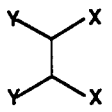

X, Y = O, N, S

have a remarkable efficiency for propagating an antiferromagnetic interaction between two paramagnetic metal ions relatively far from each other.[6,7,26,27] The molecular orbitals of the bridging species interact with the d metal orbitals in which the unpaired electrons reside. The larger the interaction, the greater is the antiferromagnetic coupling. Two main factors govern this interaction: (i) the energy difference between the symmetry-adapted bridging molecular orbitals and the d metal orbitals and (ii) the overlap between them. The influence of these parameters has been thoroughly studied by Verdaguer et al. for the bridge schematized above.[6] The oxamido bridge is especially efficient in propagating the interaction. On one hand, the lower electronegativity of nitrogen with respect to oxygen leads to a gap between the oxamido bridge molecular orbitals and the d metal orbitals smaller than the corresponding gap with an oxalato bridge. On the other hand, the metal–nitrogen and metal–oxygen distances are very close, but shorter than the metal–sulfur one, and contribute to maintaining a good overlap between the bridge and d metal orbitals. Thus, the oxamido bridge exhibits the best compromise between the two parameters controlling the exchange interaction. This leads to large values ($J = -101.0$ and -26.6 cm^{-1}) of the coupling constants for [Cu_3Ni] and [Cu_3Mn]. To understand the smaller J value observed for [Cu_3Mn], we have to take into account the number of unpaired electrons. The expected relation between the two coupling constants is $J_{CuNi} \approx 2.5J_{CuMn}$, everything being equal.[31] However, three others factors must be considered: (i) the M(II)–O distance is usually larger for Mn than for Ni; (ii) the energies of the 3d Mn(II) orbitals are higher than the corresponding ones for Ni(II), leading to a smaller interaction with the symmetry-adapted bridging molecular orbitals; (iii) there are a larger number of ferromagnetic contributions for [Cu_3Mn] (5) when compared to [Cu_3Ni] (2). All these factors cause a decrease in the expected value for the [Cu_3Mn] coupling constant and lead to the observed relation between the two parameters $J_{CuNi} \approx 4J_{CuMn}$.

The remarkable efficiency of the oxamido bridge in transmitting the interaction between two metal ions separated by more than 5 Å is not enough to explain the magnitude of the exchange interaction for [Cu_3Cd]. The presence of the cadmium ion among the copper ions could be the clue. The cadmium $d_{x^2-y^2}$ and d_{z^2} orbitals overlap the oxamido bridge orbitals. This interaction leads to new molecular orbitals, some of which are higher in energy than the oxamido bridge molecular orbitals. The higher the energy of the bridge molecular orbitals is, the larger the antiferromagnetic coupling.

The ground-state spin values of the [Cu_3Ni] and [Cu_3Mn] compounds are the result of two factors: (i) the topology of the molecule and (ii) the spin value of outer and central metal ions. Whatever the nature of the interaction (antiferromagnetic or ferromagnetic), the molecular topology imposes the condition that the spins of the three copper ions point in the same direction, leading to an effective ferromagnetic interaction between them with $S^* = S_{Cu1} + S_{Cu2} + S_{Cu3} = {}^3/_2$. This is true whenever the interaction between the central and the outer ions is greater than that between the outer ions themselves. The observed ground states for [Cu_3Mn] and [Cu_3Ni] have the expected spin arrangement ($S^* = {}^3/_2$). For [Cu_3Mn], the magnetic data at low temperature confirm that the ground state is a triplet and the only possible triplet state for this complex arises from the coupling between $S^* = {}^3/_2$ and $S_{Mn} = {}^5/_2$. For [Cu_3Ni], the magnetic susceptibility shows that the ground state is a doublet in the 25–4 K temperature range. There are two possible doublet states, one with $S^* = {}^3/_2$ and the other with $S^* = {}^1/_2$. But as shown in the EPR section (vide supra), the average g value of 2.01 confirms that the observed doublet is the one with $S^* = {}^3/_2$. Indeed, from eq 8 the expected value for the other doublet is calculated as

$$g_{1/2,1/2} = \frac{4g_{Ni} - g_{Cu}}{3} \qquad (18)$$

which would lead to a $g_{1/2,1/2}$ value close to 2.2.

This effective ferromagnetic coupling between the outer ions, even when all nearest neighbors are antiferromagnetically coupled, is highly interesting in the context of synthesizing high-spin molecules. For this purpose, the best result would be obtained in a topology where a maximum number of spins point in the same direction, as is the case for [Cu_3Ni] and [Cu_3Mn]. The other two possibilities, namely the square and the linear arrangements, lead, in the case of identical ions, to a diamagnetic ground state due to the equal number of spins in each direction, as illustrated by the following schemes:

(26) (a) Felthouse, T. R.; Laskowski, E. J.; Hendrickson, D. N. *Inorg. Chem.* **1977**, *16*, 1077. (b) Verdaguer, M.; Julve, M.; Michalowicz, A.; Kahn, O. *Inorg. Chem.* **1983**, *22*, 2624. (c) Julve, M.; Kahn, O. *Inorg. Chim. Acta* **1983**, *76*, L39. (d) Julve, M.; Faus, J.; Verdaguer, M.; Gleizes, A. *J. Am. Chem. Soc.* **1984**, *106*, 8306. (e) Ribas, J.; Montfort, M.; Diaz, C.; Solans, X. *An. Quim.* **1988**, *B84*, 186. (f) Battaglia, L. P.; Bianchi, A.; Corradi, A. B.; Garcia-Espana, E.; Micheloni, M.; Julve, M. *Inorg. Chem.* **1988**, *27*, 4174.
(27) Bencini, A.; Benelli, C.; Gatteschi, D.; Zanchini, C.; Fabretti, A.; Franchini, G. *Inorg. Chim. Acta* **1984**, *86*, 169.
(28) (a) Girerd, J. J.; Jeannin, S.; Jeannin, Y.; Kahn, O.; Lavigne, G. *Inorg. Chem.* **1978**, *17*, 3034. (b) Chauvel, C.; Girerd, J. J.; Jeannin, Y.; Jeannin, S.; Kahn, O. *Inorg. Chem.* **1979**, *18*, 3015. (c) Veit, R.; Girerd, J. J.; Kahn, O.; Robert, F.; Jeannin, Y.; El Murr, N. *Inorg. Chem.* **1984**, *23*, 4448.
(29) Vicente, R.; Ribas, J.; Alvarez, S.; Solans, X.; Fontalba, M.; Verdaguer, M. *Inorg. Chem.* **1987**, *26*, 4004.
(30) Julve, M.; De Munno, G.; Bruno, G.; Verdaguer, M. *Inorg. Chem.* **1988**, *27*, 3160.
(31) (a) Girerd, J. J.; Charlot, M. F.; Kahn, O. *Mol. Phys.* **1977**, *34*, 1063. (b) Tola, P.; Kahn, O.; Chauvel, C.; Coudanne, H. *Nouv. J. Chem.* **1977**, *1*, 467.

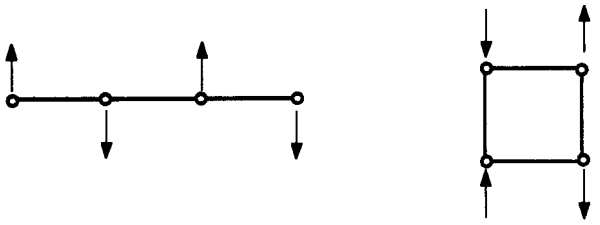

This quite simple topological approach could be formalized in terms of graph theory.[32]

The best design for polymetallic complexes containing n ions is the graph where one point has a degree equal to $n - 1$ and all the others have a degree equal to 1. This rule leads to the following graphs for n = 3-5:

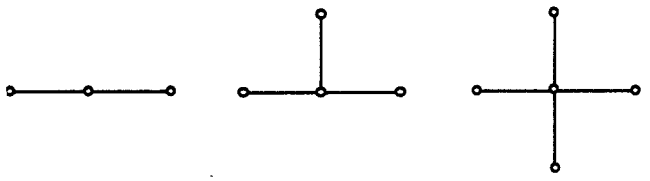

The challenge for the chemist is to find real molecules having these topologies. In this respect, inorganic compounds offer the unique possibility of choosing the spin value for each point of the graph by changing the nature of the interacting ions. For $[Cu_3Ni]$ and $[Cu_3Mn]$ the smaller $S = {}^1/_2$ spins are located outside with the largest spin at the center, yielding low-spin multiplicities overall. But if one could synthesize a molecule with a reverse of this arrangement, a high-spin ground state would be reached. We have already had some success along this line in the case of trinuclear species with the synthesis of a linear $Mn^{II}Cu^{II}Mn^{II}$ complex having a $S = {}^9/_2$ ground state.[33]

To conclude, molecular topology is a very important factor determining the magnetic properties of polynuclear complexes with more than two metal ions. It is significant that the actual geometry does not govern the spin structure. For instance, the three-dimensional compounds studied in this article and the planar trimethylenemethane biradical have the same topology and consequently the same spin structure. Thus it is possible to tune the magnetic properties of the polynuclear complex by controlling the topology and the nature of the ions in interaction. This approach is particularly promising for the synthesis of high-spin molecules.

Safety Note. Perchlorate salts of metal complexes with organic ligands are potentially explosive. In the syntheses described here we used only small amounts of material (the preparations were carried out at the millimole scale) and the starting perchlorate salt was an aquo complex. The dilute solutions were handled with great caution and evaporated slowly at room temperature.[34] When noncoordinating agents are required, every attempt should be made to substitute anions such as the fluoro sulfonates for the perchlorates.

Acknowledgment. This work was partially supported by the "Proyecto Prioritario Hispano-Francês No. 52" and the Comisiôn Interministerial de Ciencia y Technologia (Proyecto PB88-0490).

(32) Hansen, P. J.; Jurs, P. C. *J. Chem. Educ.* **1988**, *65*, 574.

(33) Yu, P.; Journaux, Y.; Kahn, O. *Inorg. Chem.* **1988**, *27*, 399.

(34) (a) *J. Chem. Educt.* **1973**, *50*, A335. (b) *Chem. Eng. News* **1983**, *61* (Dec 5), 4; **1963**, *41* (July 8), 47. (c) *J. Chem. Educ.* **1985**, *62*, 1001.

Contribution from the Department of Chemistry, Loyola University of Chicago, Chicago, Illinois 60626, and Department of Pediatrics, College of Medicine, University of Illinois at Chicago, Chicago, Illinois 60612

Comparison of Li^+ Transport and Distribution in Human Red Blood Cells in the Presence and Absence of Dysprosium(III) Complexes of Triphosphate and Triethylenetetraminehexaacetate[1]

Duarte Mota de Freitas,*,† Maryceline T. Espanol,† Ravichandran Ramasamy,† and Richard J. Labotka‡

Received November 14, 1989

Discrimination between intra- and extracellular Li^+ pools in Li^+-loaded human red blood cells (RBCs) was achieved by two distinct ^7Li NMR methods. One NMR method involved the incorporation in the RBC suspension of cell-impermeable shift reagents, either $Dy(PPP)_2^{7-}$ (dysprosium(III) triphosphate) or $Dy(TTHA)^{3-}$ (dysprosium(III) triethylenetetraminehexaacetate), and recording a standard one-dimensional FT-NMR spectrum of the $^7Li^+$ nucleus. The other NMR approach took advantage of the different relaxation properties of the two Li^+ pools and involved a modified inversion recovery (MIR) pulse sequence. We investigated the effect of $Dy(PPP)_2^{7-}$ and $Dy(TTHA)^{3-}$ on the transmembrane Li^+ distribution ratio ($[Li^+]_{RBC}/[Li^+]_{plasma}$) and on the rates of Na^+-Li^+ countertransport in Li^+-loaded human RBC by the two NMR techniques and by atomic absorption (AA) spectrophotometry, an invasive approach commonly used in clinical studies. The Li^+ transport parameters measured in the absence of shift reagents by MIR and AA or in the presence of $Dy(TTHA)^{3-}$ by ^7Li NMR spectroscopy or AA correlated significantly. However, the Li^+ transport rates measured in the presence of $Dy(PPP)_2^{7-}$ by ^7Li NMR spectroscopy or AA were higher than those measured in the presence of $Dy(TTHA)^{3-}$ or in the absence of shift reagents; the Li^+ RBC transmembrane ratios measured in the presence of the triphosphate shift reagent were higher than those measured in the two other suspension media under the same conditions. In contrast, the Na^+ distribution ratios measured in the presence of $Dy(PPP)_2^{7-}$ by ^{23}Na NMR spectroscopy or AA were lower than those measured in the presence of $Dy(TTHA)^{3-}$ or in the absence of shift reagents. Although both ^7Li NMR methods have distinct advantages over AA, such as visualization of Li^+ transport and no requirement for cell lysis, the incorporation of $Dy(PPP)_2^{7-}$ in the cell suspension changed the Li^+ transport rates and ratios in RBCs and must be used with caution.

Introduction

Lithium salts are the preferred drugs in the treatment and maintenance of both manic and depressive episodes in psychiatric patients with bipolar affective disorders (or manic-depressive disorders as they were formerly called).[2] Lithium has also been used in a variety of other psychiatric and medical conditions,

(1) This paper was presented in part at the International Symposium on Biological and Synthetic Membranes, Lexington, KY, Oct 1988. A book chapter appeared in the conference proceedings: Espanol, M. T.; Ramasamy, R.; Mota de Freitas, D. In *Biological and Synthetic Membranes*; Butterfield, D. A., Ed.; Alan R. Liss: New York, 1989; pp 33-43.

* To whom correspondence should be addressed.
† Loyola University of Chicago.
‡ University of Illinois.

0020-1669/90/1329-3972$02.50/0